LOWER EMITTANCE LATTICE FOR THE ADVANCED PHOTON SOURCE UPGRADE USING REVERSE BENDING MAGNETS*

M. Borland, Y. Sun, V. Sajaev, R. R. Lindberg, T. Berenc, ANL, Argonne, IL 60439, USA

Abstract

The Advanced Photon Source (APS) is pursuing an upgrade to the storage ring to a hybrid seven-bend-achromat design [1]. The nominal design provides a natural emittance of 67 pm [2]. By adding reverse dipole fields to several quadrupoles [3, 4] we can reduce the natural emittance to 41 pm while simultaneously providing more optimal beta functions in the insertion devices and increasing the dispersion function at the chromaticity sextupole magnets. The improved emittance results from a combination of increased energy loss per turn and a change in the damping partition. At the same time, the nonlinear dynamics performance is very similar, thanks in part to increased dispersion in the sextupoles. This paper describes the properties, optimization, and performance of the new lattice.

INTRODUCTION

APS is pursuing a major upgrade of our 7-GeV storage ring, replacing the double-bend structure with a 6-GeV multi-bend achromat [5] in order to achieve much lower emittance. The nominal lattice, based on a hybrid seven-bend achromat [1], achieves a natural emittance of 67 pm [2] and reasonable nonlinear dynamics performance [2, 6, 7]. In an effort to reduce the emittance further, we explored the option of converting several quadrupoles into combined-function weak reverse bending magnets [3, 4].

The use of reverse bends (RBs) has several potential advantages: it increases the energy loss per turn, thus potentially reducing emittance much as a damping wiggler would; it allows manipulation of the damping partition numbers; it provides additional means of manipulating the dispersion function; and it reduces constraints on the lattice quadupoles, potentially allowing more optimized beta functions at the straight sections.

LINEAR OPTICS

Linear optics design started from the 67-pm lattice. The four quadrupoles in the high-dispersion region and the central FODO-like region were all converted into gradient dipoles with zero bending angle. The parallel hybrid simplex optimizer [8] in `Pelegant` [9, 10] was then allowed to vary the angles of both the normal and reverse bending dipoles and the quadrupole gradients. After several iterations, it became clear that only three of the RBs were in fact effective, namely, those replacing the central two quadrupoles in each high-dispersion region and the central two quadrupoles in the FODO region; this is a total of six RBs per sector. Instead of merely attempting to minimize the emittance, we attempted to maximize the approximate brightness for an 18-mm-period, 3.7-m-long superconducting undulator tuned for 20 keV at the 3^{rd} harmonic. This automatically incorporates the fact that maximizing brightness depends not only on lowering the emittance, but also on having closer-to-ideal beta functions. The lattice functions are shown in Fig. 1, while Table 1 lists several properties of the lattice in comparison to the 67-pm lattice. In addition to the significantly lower emittance, the beta functions at the IDs are both smaller, which further enhances the x-ray brightness. The maximum dispersion is 20% larger, which helps reduce the strength of the sextupoles.

Table 1: Comparison of the 67-pm and 41-pm lattices.

	67pm	41pm
ν_x	95.125	95.091
ν_y	36.122	36.165
$\xi_{x,nat}$	-139	-130
$\xi_{y,nat}$	-108	-123
Nat. emittance (pm)	66.9	41.4
Energy spread (%)	0.096	0.129
Horiz. damping time (ms)	12.1	7.2
Long. damping time (ms)	14.1	19.6
Energy loss (MeV/turn)	2.27	2.80
Momentum compaction	5.7×10^{-5}	3.8×10^{-5}
Damping partition J_x	1.61	2.20
Damping partition J_δ	1.39	0.80
Max. η_x (m)	0.074	0.090
@ ID Straight Sections:		
β_x (m)	7.0	4.9
η_x (mm)	1.11	1.47
β_y (m)	2.4	1.9
$\epsilon_{x,eff}$ (pm)	67.0	41.8

NONLINEAR DYNAMICS OPTIMIZATION

Nonlinear dynamics optimization was performed using a tracking-based multi-objective genetic algorithm (MOGA) [11, 12] (similar to [13, 14]) based on dynamic acceptance (DA) and Touschek lifetime obtained from the local momentum acceptance (LMA) [15, 16]. One refinement is that the rf voltage is adjusted for each trial configuration to be no larger than the maximum LMA, which ensures the lowest voltage and longest bunch possible.

As with the 67-pm lattice, the DA is only large enough for on-axis injection, but the LMA is larger, approaching ±5% in some cases. The momentum tune footprint of the

* Work supported by the U.S. Department of Energy, Office of Science, Office of Basic Energy Sciences, under Contract No. DE-AC02-06CH11357.

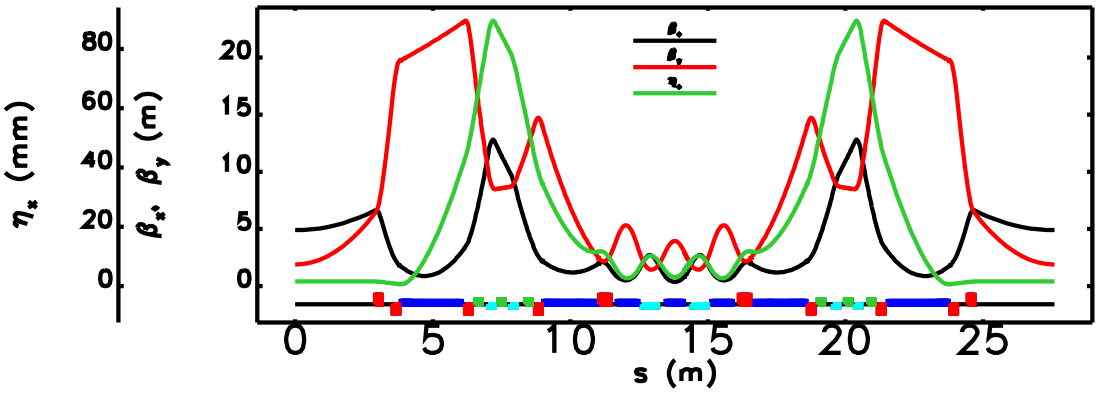

Figure 1: Lattice functions for the 41-pm lattice with reverse bends. Dipoles are blue (normal) and cyan (reverse), quadrupoles are red, and sextupoles are green.

67-pm lattice is compared to several variants of the 41-pm lattice in Fig. 2 Several strategies were tried in MOGA to obtain these variants: (1) Independent sextupoles in odd and even sectors without translation symmetry. (2) Same, but translation-symmetry within a sector. Also, based on robustness tests (similar to [2]) we added a momentum tune footprint constraint for $\delta : [-4, 4]\%$ to delay crossing the integer resonance, rather than simply minimizing the tune footprint, which we found previously to cause poor LMA in the high-dispersion regions. (3) Same as (1), but with tune footprint optimization included. (4) Same as (3), but tune footprint momentum range increased to $\delta : [-5, 5]\%$.

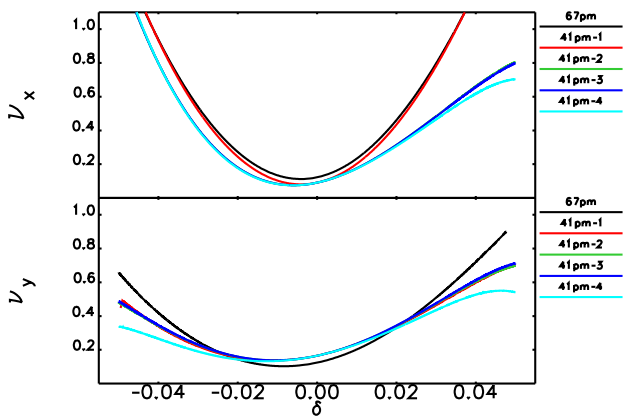

Figure 2: Momentum tune footprints for several variants of the 41-pm lattice compared to the 67-pm lattice.

EVALUATION

The several lattice variants were subjected to ensemble evaluation, which begins with simulated commissioning [17]. The corrected error ensembles include misalignments and strength errors, as well as simulated corrections to the orbit, tunes, chromaticities, lattice functions, and coupling. The 100 corrected ensembles are used in computation of DA, LMA, lattice functions, and the emittance ratio. Figure 3 compares the 10^{th}-percentile DA contours of the four lattices. Also shown is the 2σ beam size from the injector, where the size includes both the actual beam size as well as assumed trajectory jitter. We see that the increased emphasis on momentum detuning in variants 2,3, and 4 comes at a cost in terms of DA, but the latter is still larger than the effective injected beam size. Simulation of injection efficiency is planned to verify the adequacy of the DA.

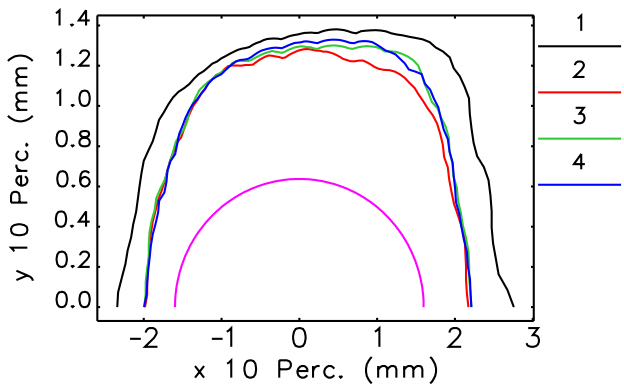

Figure 3: 10^{th}-percentile DA contours for four variants of the 41-pm lattice.

The ensemble emittance ratio data is used as input to computation of intrabeam scattering (IBS) using `ibsEmittance`, assuming use of an optimized 4^{th} harmonic bunch lengthening cavity (BLC). The IBS-inflated beam parameters are then used together with the LMA in computation of the Touschek lifetime using `touschekLifetime` [18]. This is a simpler and much faster, but less precise, method than described in [6]. It underestimates the Touschek lifetime because in reality the BLC can be tuned past the nominal optimum, producing a double-humped time profile and longer Touschek lifetime. Figure 4 compares the Touschek lifetime distributions for the four variants in 200-mA, 324-bunch, round-beam mode, showing a 60% increase for the new variants.

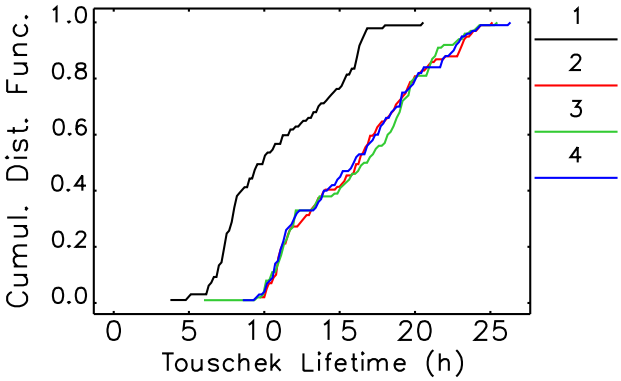

Figure 4: Cumulative distributions of Touschek lifetime for four variants of the 41-pm lattice, for 200 mA in 324 bunches with $\epsilon_x = \epsilon_y$.

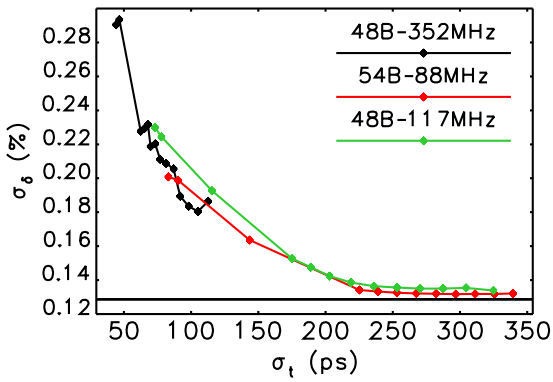

Figure 5: Predicted energy spread as a function of rms bunch length, where the bunch length is changed by varying the detuning of passive bunch-lengthening cavities.

BENEFITS OF LOW-FREQUENCY RF

The MAX-IV light source [19] uses an rf frequency of 100 MHz, which allows for much longer bunches, with benefits in suppression of IBS and improvement of Touschek lifetime [20]. Because the Touschek lifetime for APS-U is not as long as we would like, we have investigated the implications of replacing our existing 352-MHz, $h = 1296$ system with a similar low-frequency system.

One option is to retain several 352-MHz cavities for use as bunch lengthening cavities; in that case, we have a choice of moving to 88 MHz ($h = 324$) or 117 MHz ($h = 432$) as our main rf frequency. 88 MHz has the disadvantage of not supporting a uniform 48-bunch fill, which is our planned timing mode; using fewer bunches is not considered possible for the injector, while using more bunches will increase the difficulty of timing experiments. On the other hand, 117 MHz has the disadvantage of not supporting a uniform 324-bunch fill, which is our planned many-bunch mode; the number of bunches in this mode is limited by fast kicker performance, leaving 216 bunches as the best alternative. This will partly undo the beneficial effects of the low-frequency system by forcing the use of higher-charge bunches. However, this is the best choice given that the lifetime of the 48-bunch mode is the greatest concern. Figure 5 shows tracking results for possible timing modes including the longitudinal impedance, showing the beneficial effect on the energy spread due to suppression of the microwave instability (MWI), which is included using the impedance model [21, 22]. In addition, IBS is suppressed, resulting in a reduction of the emittance by about 6%. As Fig. 6 shows, the lifetime increases by about a factor of 2..

Alternatively, we could ignore the existing rf systems and pick the best frequency based on other considerations. This would entail extra expense and risk to design and build a new BLC, as the existing 352-MHz cavities could not be used. We performed an analyis of the Pareto-optimal choices for the rf harmonic, attempting to maximize the number of available uniform bunch modes, get close to a 48-bunch mode, and get close to a 324-bunch mode. On this basis, several other harmonic numbers suggest themselves, particularly $h = 336$ (91 MHz) and $h = 480$ (130 MHz).

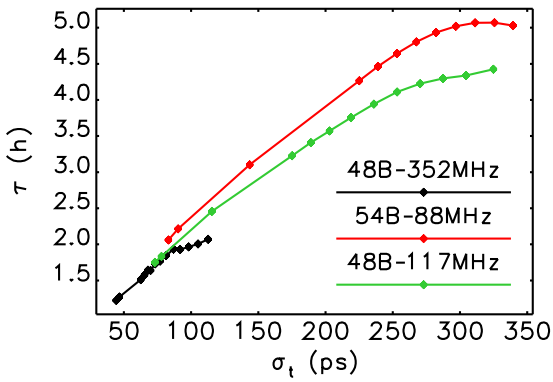

Figure 6: 10^{th}-percentile beam lifetime as a function of rms bunch length for various fundamental rf frequency choices. A gas-scattering lifetime of 60 h is included [23].

CONCLUSIONS

A 41-pm hybrid seven-bend achromat lattice with six reverse-direction bending magnets per sector has been developed as a candidate for the APS upgrade. The lattice provides a 50% increase in x-ray brightness compared to the 67-pm lattice, with comparable dynamic acceptance and lifetime. Lifetime may be increased and IBS/MWI suppressed using a low-frequency rf system.

ACKNOWLEDGMENTS

Computations made use of Blues, a high-performance computing cluster operated by the Laboratory Computing Resource Center at Argonne National Laboratory.

REFERENCES

[1] L. Farvacque *et al.*, in *Proc. 2013 IPAC*, 2013, p. 79.

[2] M. Borland *et al.*, in *Proc. IPAC15*, pp. 1776-1779.

[3] J. Delahaye *et al.*, in *Proc. PAC89*, pp. 1611-1613.

[4] A. Streun. *NIM A*, vol. 737, p. 148, 2014.

[5] D. Einfeld *et al.*, *NIM-A*, vol 335, p. 402, 1993.

[6] A. Xiao *et al.*, in *Proc. IPAC15*, pp. 599-561.

[7] A. Xiao *et al.*, in *Proc. IPAC15*, pp. 1816-1818.

[8] Y. Wang *et al.*, in *Proc. PAC 2011*, pp. 787-789.

[9] M. Borland. ANL/APS LS-287, Advanced Photon Source, 2000.

[10] Y. Wang *et al.*, in *Proc. PAC 2007*, pp. 3444-3446.

[11] M. Borland *et al*,. ANL/APS/LS-319, APS, 2010.

[12] M. Borland *et al.*, *J Synchrotron Radiation*, vol. 21 p. 912 2014.

[13] K. Deb *et al.*, *IEEE TEC*, vol. 6 p. 182, 2002.

[14] I. Bazarov *et al.*, *Phys Rev ST Accel Beams*, vol. 8 p. 034202, 2005.

[15] C. Steier *et al.*, *Phys Rev E*, vol. 65 p. 056506, 2002.

[16] M. Belgrounne *et al.*, in *Proc. PAC 2003*, pp. 896–898.

[17] V. Sajaev *et al.*, in *Proc. IPAC15*, pp. 553-555.

[18] A. Xiao *et al.*, in *Proc. PAC 2007*, pp. 3453-3455.

[19] P. Tavares *et al.*, presented at NAPAC 2016, this conference.

[20] S. C. Leemann, *Phys Rev ST Accel Beams*, vol. 17 p. 050705, 2014.

[21] R. R. Lindberg *et al.*, in *Proc. IPAC15*, pp. 1825-1827.

[22] R. R. Lindberg *et al.*, presented at NAPAC 2016, paper TUPJE077, this conference.

[23] M. Borland *et al.*, in *Proc. IPAC15*, pp. 546-549.